

Large-scale synthesis and field emission properties of vertically oriented CuO nanowire films

Y W Zhu^{1,2}, T Yu¹, F C Cheong¹, X J Xu^{3,4}, C T Lim^{3,4},
V B C Tan^{3,4}, J T L Thong^{3,5} and C H Sow^{1,2,6}

¹ Department of Physics, Blk S12, National University of Singapore, 2 Science Drive 3, 117542, Singapore

² National University of Singapore Nanoscience and Nanotechnology Initiative, Blk S13, 2 Science Drive 3, 117542, Singapore

³ National University of Singapore Nanoscience and Nanotechnology Initiative, Blk E3, 2 Engineering Drive 3, 117576, Singapore

⁴ Department of Mechanical Engineering, National University of Singapore, 9 Engineering Drive 1, 117576, Singapore

⁵ Center for Integrated Circuit Failure Analysis and Reliability, Faculty of Engineering, National University of Singapore, 4 Engineering Drive 3, 117576, Singapore

E-mail: physowch@nus.edu.sg (C H Sow)

Received 25 August 2004, in final form 19 October 2004

Published 2 December 2004

Online at stacks.iop.org/Nano/16/88

Abstract

Using a simple method of direct heating of bulk copper plates in air, oriented CuO nanowire films were synthesized on a large scale. The length and density of nanowires could be controlled by growth temperature and growth time. Field emission (FE) measurements of CuO nanowire films show that they have a low turn-on field of 3.5–4.5 V μm^{-1} and a large current density of 0.45 mA cm^{-2} under an applied field of about 7 V μm^{-1} . By comparing the FE properties of two types of samples with different average lengths and densities (30 μm , 10⁸ cm^{-2} and 4 μm , 4 $\times 10^7$ cm^{-2} , respectively), we found that the large length–radius ratio of CuO nanowires effectively improved the local field, which was beneficial to field emission. Verified with finite element calculation, the work function of oriented CuO nanowire films was estimated to be 2.5–2.8 eV.

1. Introduction

Recently, quasi-one-dimensional (1D) nanomaterials have attracted much attention because of their unique properties and potential applications [1]. Since the sharp tips of 1D nanostructures can effectively enhance local electric fields, using them as field emission cathodes is a promising way to obtain high brightness electron sources and to fabricate field emission displays (FEDs) [2]. Among the 1D materials, carbon nanotubes (CNTs) are studied extensively [3] because of their high aspect ratio and unique electrical and mechanical properties. However, further development of FE emitters depends critically on the challenging task of growing CNTs with specific properties [4]. On the other hand, a number of

researchers have been actively looking for alternative materials as FE emitters [5].

Among the different types of 1D nanostructures considered for use as narrow gap semiconductors (1.2 eV) [6], CuO nanostructures have interested several research groups [6–9]. Jiang *et al* used the vapour-phase approach to synthesize CuO nanowires with lengths of up to 15 μm on surfaces of various copper substrates [6]. Recently, Chien *et al* grew a variety of CuO nanostructures [7] and measured their FE properties [8]. This pioneering work showed that the work function of CuO nanofibres can be as low as 0.3–2.62 eV. However, in the reported literature [7–9], the synthesis of aligned CuO nanostructures is rather complicated and the FE turn-on fields are still as high as 6–7 V μm^{-1} [8] and ~ 11 V μm^{-1} [9], which may limit the application of CuO nanostructures as FE emitters. In this paper, we report a very simple method to synthesize

⁶ Author to whom any correspondence should be addressed.

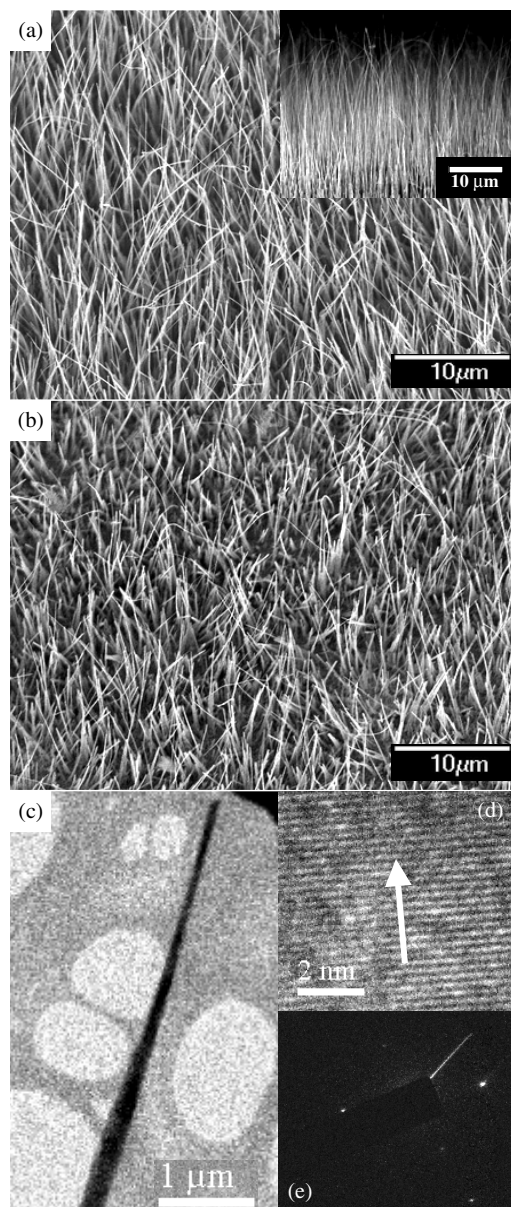


Figure 1. SEM images of CuO nanowires of type I (a) and type II (b) with sample tilting angle of 15° during imaging. The inset of (a) shows a side view of nanowires of type I. We can see that the nanowires are well aligned. (c) TEM image of one single tip of the type II samples. (d) HRTEM image showing the crystalline nanowire. The lattice fringe spacing is about 0.247 nm, which is consistent with the $\{111\}$ planes in monoclinic CuO as shown by the arrow. (e) Electron diffraction pattern that is typically observed [6]. The electron beam was parallel to the $[110]$ direction.

uniform, extended and oriented CuO nanowire films. Using as-grown samples as FE cathodes, we found that they have low turn-on field, high current density and uniform emission over a large area. Also, by comparing the finite element calculation and experimental results, the work function of the CuO nanowire films was estimated to be 2.5–2.8 eV.

2. Experimental details

Oriented CuO nanowire films were prepared in ambient atmosphere by using a simple vapour–solid reaction

method [10]. The substrate is a copper plate (99.999% purity, Sigma-Aldrich Pte. Ltd) with thickness of 0.5 cm and size of $10\text{ cm} \times 3\text{ cm}$. Before growth, sandpaper (320 grits) was used to remove oxide layers on the surface. The Cu plate was then heated on a hotplate under ambient conditions. The growth temperature was about $390\text{--}430^\circ\text{C}$ and the growth time varied from one day to three days, during which a black layer was formed on the substrate. After cooling, this layer was peeled off carefully and characterized using scanning electron microscopy (SEM, JEOL JSM-6400F) and transmission electron microscopy (TEM, JEOL JEM-2010F, 300 kV).

3. Result and discussions

Two typical morphologies were analysed. One was prepared at 390°C with growth time of three days (type I); the other type was grown after heating for one day at 430°C (type II). Figures 1(a) and (b) show the SEM images of type I and II CuO nanowires, respectively. The inset of figure 1(a) shows a side view of the type I samples. From the images, we can see that both types of vertically oriented CuO nanowires have sharp tips, which is beneficial to field emission. It can also be seen that the type I nanowires, with an average density of about 10^8 cm^{-2} , have an average length of $30 \pm 3\ \mu\text{m}$ and a diameter of $60 \pm 15\text{ nm}$ at the tips. Type II samples have an average density of about $4 \times 10^7\text{ cm}^{-2}$, an average length of $4 \pm 0.7\ \mu\text{m}$ and a typical tip diameter of $90 \pm 10\text{ nm}$. Figure 1(c) shows a TEM image of a nanowire from a type II sample, from which we can see the sharp tip more clearly. Figures 1(d) and (e) are a high resolution TEM (HRTEM) image and selected area electron diffraction (SAED) pattern showing that the nanowires are crystalline. The interplanar distance of fringes parallel to the wire axis is 0.247 nm, corresponding to the $[\bar{1}11]$ direction of monoclinic CuO.

The measurements of FE properties of the two types of CuO nanowire films were carried out using a two-parallel-plate configuration in a vacuum chamber with a pressure of about $5 \times 10^{-7}\text{ Torr}$. The peeled nanowire films were adhered onto a Cu substrate cathode by copper double-sided tape. Indium tin oxide (ITO) glass covered with a layer of phosphor was employed as the anode. A cover glass was used as a spacer and the distance between electrodes was kept at $150\ \mu\text{m}$. A Keithley 237 high voltage source measurement unit (SMU) was used to apply a voltage from 0 to 1100 V and to measure the emission current at the same time. All the measurements were performed at room temperature.

Figure 2(a) shows the typical current density–electric field (J – E) curves of the two types of CuO nanowire films. It can be seen that the type I nanowires have a very low turn-on field of $3.3\text{ V}\ \mu\text{m}^{-1}$ and those of type II still have a relatively low turn-on field of $4.5\text{ V}\ \mu\text{m}^{-1}$, compared with previous reports [8, 9]. Repeated experiments demonstrated that the turn-on fields of CuO nanowire films mainly fall between 3.5 and $4.5\text{ V}\ \mu\text{m}^{-1}$. Also, the maximum current density of both types can be as high as $0.45\text{ mA}\ \text{cm}^{-2}$ (under a field of $7\text{ V}\ \mu\text{m}^{-1}$), which is comparable with some results achieved with CNT emitters [11]. At the same time, uniform FE images were observed, which are shown in figures 2(b) and (c). The inset of figure 2(a) shows the corresponding Fowler–Nordheim

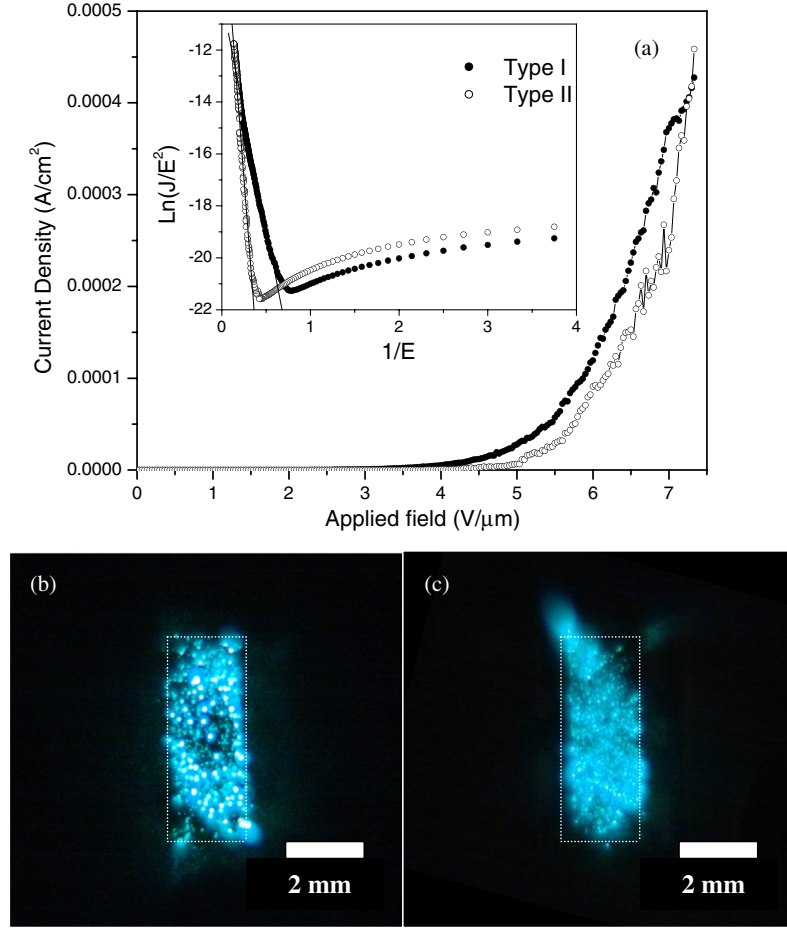


Figure 2. (a) Field emission J - E curves from the CuO nanowire films of two typical morphologies. The inset depicts the FN plot; the linear dependence indicates that the emission satisfies the FN mechanism. (b), (c) Fluorescence field emission images of CuO nanowires of type I (b) and type II (c) under an applied voltage of 1000 V. The dotted rectangles represent the boundaries of the samples. (This figure is in colour only in the electronic version)

(FN) plots of the CuO nanowires. We can see that at high fields the linear relationship between $\ln(J/E^2)$ and $1/E$ suggests that the quantum tunnelling mechanism is responsible for the emission from both types of nanowires [12].

The FN equation that is often used to analyse field emission properties can be written as [12, 13]

$$J = \frac{1.54 \times 10^{-6} F^2}{\phi} \exp\left[-\frac{6.44 \times 10^7 \phi^{3/2}}{F}\right], \quad (1)$$

where J is the emission current density (A cm^{-2}), F is the local field intensity (V cm^{-1}) and ϕ is the work function of emitters (eV). Using the concept of field enhancement factor $\beta = F/E$, where E is applied field, the slope of measured $\ln(J/E^2)$ versus $1/E$ plot can be expressed as

$$S = -6.44 \times 10^3 \frac{\phi^{3/2}}{\beta}, \quad (2)$$

where the unit of E has been changed to $\text{V } \mu\text{m}^{-1}$. The values of S for type I and II nanowires can be obtained by fitting the FN curves to the experimental results. In this work, for each type of nanowire films, five samples with relatively uniform emission images were analysed. Since two types of CuO nanowires

were synthesized with an excellent uniformity on a large scale, quite similar values of FN slopes were obtained from different samples of each type. A summary of the two groups of FN slope values is presented in table 1. It can be seen from the table that for the same type of film, the FN slopes as measured from five samples are consistent with each other. Average slope values of 16.8 ± 0.8 and 41.7 ± 3.0 were obtained for the type I and II samples, respectively. In the field emission of nanomaterials, work function is an important parameter which is difficult to define [8, 14]. Also, in the normal field emission experiments involving only one type of samples, it is quite hard to independently identify the work function and the enhancement factor. Our approach of measuring FE from two types of films from the same material provides a unique opportunity to carry out a more refined analysis of the experimental data. Reasonably assuming that the two types of samples have the same work function, we obtained the ratio of field enhancement factor of the type I sample (β_1) to that of the type II sample (β_2)

$$\gamma = \beta_1/\beta_2 = S_2/S_1 = 2.5 \pm 0.3, \quad (3)$$

where S_1 and S_2 are the slopes of FN plots for type I and for type II samples, respectively.

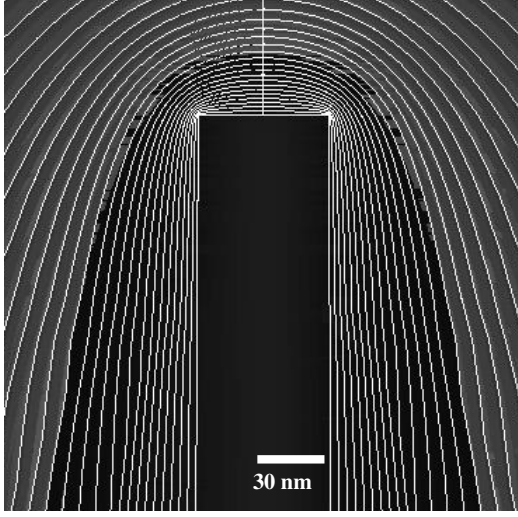


Figure 3. Finite element calculation showing equipotential lines near the tip of a single emitter based on the dimension and morphology of type I nanowires. Defining the nanowire as minus high potential and anode (not shown) as zero potential, the darker grey scale represents a lower potential area. We can see that large local field exists on both the tip and side area of the emitter.

Table 1. Measured gradients of the FN plots for five different samples corresponding to each type of CuO nanowire films.

Type	S1	S2	S3	S4	S5	Mean	Standard deviation
I	15.5	17.3	16.7	16.8	17.6	16.8	0.8
II	44.3	37.0	41.9	40.8	44.3	41.7	3.0

Since the value of β is mainly related to the geometry of emitters, we used a finite element method (ANSYS, Ansys Inc.) to grossly calculate the local field of a single emitter under a certain applied field typically used in field emission experiments. The modelling was also based on the typical morphologies and dimensions of both types of nanowires in our experiments. The calculated equipotential lines near the tip are shown in figure 3, from which we can see that because of the nano-scale geometry of CuO nanowires, a large local field exists not only on the tip area, but also on the side face near the tip. That is, if we only consider the field emission from top area of the tip, the effective field enhancement factor would be underestimated. Thus, for a single nanowire, we calculated the individual local field enhancement factor of all points which had considerable local field, β_{loc} , and defined an effective enhancement factor β_{eff} as $\beta_{eff} = \sum \beta_{loc} \cdot dS / A_{tip}$, where dS is the area of each element and A_{tip} is the tip area of a single nanowire. As our experimentally measured current density was obtained by averaging the total emission current on the whole sample area and only the tip area of nanowires contributed to this sample area, it is reasonable to redistribute all emission electrons including those from side walls on the tip area of a single nanowire to compare with the experimental data. Since in other nanowires [15] with similar morphologies and bulk work function with CuO nanowires, the β value can be as low as 10, here the above summation includes all contributions with $\beta_{loc} \geq 10$ for both types of nanowires. Then we obtain the approximate values of β_{eff} as

$\beta_{1,eff} \approx 21\,060$ for a type I single nanowire and $\beta_{2,eff} \approx 1160$ for that of type II. Taking into consideration the screening effect between adjacent nanowires, the enhancement factor of films can be well approximated by [16]

$$\beta = \beta_{eff} \left[1 - \exp\left(-2.3172 \frac{s}{l}\right) \right], \quad (4)$$

where s is the spacing between emitters and l is the length of emitters. Thus, taking the average spacing between nanowires as $1\ \mu\text{m}$ (corresponding to a density of about $10^8\ \text{cm}^{-2}$) for type I and $1.5\ \mu\text{m}$ (corresponding to a density of about $4 \times 10^7\ \text{cm}^{-2}$) for type II, the enhancement factors of CuO nanowire films were calculated as

$$\beta_{1,cal} = 1570 \quad \text{and} \quad \beta_{2,cal} = 670, \quad \text{respectively.} \quad (5)$$

Hence, we obtain the estimated ratio of the field enhancement factors for the two types of nanowire films as

$$\gamma_{cal} = \beta_{1,cal} / \beta_{2,cal} \approx 2.34. \quad (6)$$

This result is in very good agreement with the experimentally measured value of 2.5 ± 0.3 . Using equation (2) and results of (5) as estimated enhancement factors of samples, the work function of CuO nanowire films can be estimated as 2.5–2.8 eV, which is nearly half that of the bulk CuO work function [17] and consistent with the results of 0.3–2.62 eV as reported by Chien *et al* [8]. Of course, in our experimental conditions with the vacuum of 5×10^{-7} Torr the field emission is most likely to be dominated by adsorbate enhanced states, and not by the CuO surface work function. Similar field emission experiments in higher vacuum are currently underway to obtain a more accurate value of CuO nanowire work function.

4. Conclusions

In conclusion, large-scale oriented CuO nanowire films have been synthesized using a simple method of heating bulk Cu in air. Measurements of the FE properties of two typical morphologies show that they have low turn-on field of 3.5–4.5 $\text{V}\ \mu\text{m}^{-1}$ and high emission current density of 0.45 $\text{mA}\ \text{cm}^{-2}$ (at the field of 7 $\text{V}\ \mu\text{m}^{-1}$). At the same time, uniform FE images have been observed. By comparing the experimental data with finite element calculation results, the work function of the CuO nanowire films is estimated to be about 2.5–2.8 eV. The simple synthesis method, low turn-on voltage, high FE current density and uniform FE images make CuO nanowires one of the promising candidates as future FE electron sources and FEDs.

Acknowledgments

The authors acknowledge the foundation support from NUSARF and NUSNNI. TY thanks the Singapore Millennium Foundation for support.

References

- [1] Xia Y N, Yang P D, Sun Y G, Wu Y Y, Mayers B, Gates B, Yin Y D, Kim F and Yan H 2003 *Adv. Mater.* **15** 353
- [2] Saito Y and Uemura S 2000 *Carbon* **38** 169

- Kim J M, Choi W B, Lee N S and Jung J E 2000 *Diamond Relat. Mater.* **9** 1184
- [3] de Heer W A, Chatelain A and Ugarte D 1995 *Science* **270** 1179
- Bonard J, Kind H, Stöckli T and Nilsson L 2001 *Solid-State Electron.* **45** 893
- [4] Baughman R H, Zrkhidov A A and de Heer W A 2002 *Science* **297** 787
- [5] Zhou J, Deng S Z, Xu N S, Chen J and She J C 2003 *Appl. Phys. Lett.* **83** 2653
- Zhu Y W, Zhang H Z, Sun X C, Feng S Q, Xu J, Zhao Q, Xiang B, Wang R M and Yu D P 2003 *Appl. Phys. Lett.* **83** 144
- Jia H B, Zhang Y, Zhang X H, Shu J, Luo X H, Zhang Z S and Yu D P 2003 *Appl. Phys. Lett.* **82** 4146
- [6] Jiang X C, Herricks T and Xia Y N 2002 *Nano Lett.* **2** 1333
- [7] Hsieh C T, Chen J M, Lin H H and Shih H C 2003 *Appl. Phys. Lett.* **82** 3316
- [8] Hsieh C T, Chen J M, Lin H H and Shih H C 2003 *Appl. Phys. Lett.* **83** 3383
- [9] Chen J, Deng S Z, Xu N S, Zhang W X, Wen X G and Yang S H 2003 *Appl. Phys. Lett.* **83** 746
- [10] Yu T, Zhao X, Shen Z X, Wu Y H and Su W H 2004 *J. Cryst. Growth* **268** 590
- [11] Choi J H, Choi S H, Han J H, Yoo J B, Park C Y, Jung T, Yu S, Han I T and Kim J M 2003 *J. Appl. Phys.* **94** 487
- [12] Tang C C and Bando Y 2003 *Appl. Phys. Lett.* **83** 659
- Fowler R H and Nordheim L W 1928 *Proc. R. Soc. A* **119** 173
- [13] Gadzuk J W and Plummer E W 1973 *Rev. Mod. Phys.* **45** 487
- Bonard J M, Salvetat J P, Stöckli T, Forró L and Châtelain A 1999 *Appl. Phys. A* **69** 245
- [14] Bonard J M, Kind H, Stöckli T and Nilsson L O 2001 *Solid-State Electron.* **45** 893
- [15] Chen J, Deng S Z, She J C, Xu N S, Zhang W X, Wen X G and Yang S H 2003 *J. Appl. Phys.* **93** 1774
- [16] Jo S H, Tu Y, Huang Z P, Carnahan D L, Wang D Z and Ren Z F 2003 *Appl. Phys. Lett.* **82** 3520
- Bonard J M, Weiss N, Kind H, Stöckli T, Forró L and Châtelain A 2001 *Adv. Mater.* **13** 184
- [17] Koffyberg F P and Benko F A 1982 *J. Appl. Phys.* **53** 1173